Haghighi Borujeini et al. Egyptian Journal of Radiology and Nuclear Medicine (2021) 52:167
https://doi.org/10.1186/s43055-021-00545-7

Egyptian Journal of Radiology and Nuclear Medicine

RESEARCH Open Access

Grading of meningioma tumors based on analyzing tumor volumetric histograms obtained from conventional MRI and apparent diffusion coefficient images

Meysam Haghighi Borujeini[1], Masoume Farsizaban[2,3], Shiva Rahbar Yazdi[4], Alaba Tolulope Agbele[5], Gholamreza Ataei[6], Korosh Saber[4*], Seyyed Mohammad Hosseini[7*] and Razzagh Abedi-Firouzjah[8*]

Abstract

Background: Our purpose was to evaluate the application of volumetric histogram parameters obtained from conventional MRI and apparent diffusion coefficient (ADC) images for grading the meningioma tumors.

Results: Tumor volumetric histograms of preoperative MRI images from 45 patients with the diagnosis of meningioma at different grades were analyzed to find the histogram parameters. Kruskal-Wallis statistical test was used for comparison between the parameters obtained from different grades. Multi-parametric regression analysis was used to find the model and parameters with high predictive value for the classification of meningioma. Mode; standard deviation on post-contrast T1WI, T2-FLAIR, and ADC images; kurtosis on post-contrast T1WI and T2-FLAIR images; mean and several percentile values on ADC; and post-contrast T1WI images showed significant differences among different tumor grades ($P < 0.05$). The multi-parametric linear regression showed that the ADC histogram parameters model had a higher predictive value, with cutoff values of 0.212 (sensitivity = 79.6%, specificity = 84.3%) and 0.180 (sensitivity = 70.9%, specificity = 80.8%) for differentiating the grade I from II, and grade II from III, respectively.

Conclusions: The multi-parametric model of volumetric histogram parameters in some of the conventional MRI series (i.e., post-contrast T1WI and T2-FLAIR images) along with the ADC images are appropriate for predicting the meningioma tumors' grade.

Keywords: Meningiomas, Magnetic resonance imaging, Histogram, Grade

Background

Meningioma is one of the frequent central nervous system (CNS) tumors in adults with a prevalence of 13–26% of all intracranial neoplasms [1]. There are three subgroups of meningiomas based on the World Health Organization (WHO) classifications; grade I has the highest percentage (about 90%), grade II (moderately differentiated), and grade III (high grade or malignant) tumors have the prevalence of 5–7% and 1–3%, respectively [1].

Magnetic resonance imaging (MRI) as high contrast modality has the ability to show the soft tissues' differentiates clearly and plays an important role in diagnosis and post-treatment evaluation of meningioma tumors [2]. Various pulse sequences like "spine echo" and "spin echo-echo planar" are usually applied during MRI procedures to obtain T1-weighted, T2-weighted, and diffusion-weighted images (DWI) for illustrating CNS

* Correspondence: korosh.iut@gmail.com; mohammad.hosseini1989@yahoo.com; razzaghabedi@gmail.com
[4]Department of Medical Physics, School of Medicine, Shahid Sadoughi University of Medical Sciences, Yazd, Iran
[7]Department of Medical Physics, Faculty of Medicine, Mashhad University of Medical Sciences, Mashhad, Iran
[8]Cellular and Molecular Research Center, Yasuj University of Medical Sciences, Yasuj, Iran
Full list of author information is available at the end of the article

tumors. It has been reported that DWI is a pulse sequence that can differentiate meningioma tumors at different grades [3]. Furthermore, quantified images obtained from DWI, namely apparent diffusion coefficient (ADC), can differentiate low-grade from high-grade meningiomas [3–7] with a sensitivity of 72.9% and specificity of 73.1% [6]. In most of the previous studies, ADC was acquired by the drawing of a region of interest (ROI) through the largest cross-section of the tumor and the mean ADC value within the ROI was estimated [4, 5, 7]. However, there is a study that reported the volumetric histogram analysis of ADC values for differentiating the low-grade tumors from moderate and high-grade ones [3].

Volumetric histogram analysis of ADC can be used for differentiating the low-grade from moderate and high-grade tumors [3], a process described clearly by Just et al. [8]. Using this method, a broad spectrum of ADC parameters in three dimensions like mean, maximum, minimum, median, mode, and different ADC percentiles, as well as statistical parameters like kurtosis, and skewness can be estimated for the tumor volume [9]. A comparison of the sensitivity and specificity values reported in different studies about the grading of the CNS tumors showed that volumetric histogram analysis parameters may be more sensitive than the "conventional" ADC values obtained from ROI in a two-dimensional image [8]. Furthermore, analyzing the volumetric histogram parameters of tumor region in other weighted MRI images like the conventional T1- and T2-weighted images could be useful for detecting the tumor grade. For instance, Meyer et al. [10] reported that tumor histogram parameters of the conventional T1- and T2-weighted MRIs can reflect different histopathological features in primary CNS lymphoma.

From our literature search, no study has evaluated the volumetric histogram parameters obtained from both conventional MRI images and ADC for differentiating meningioma tumor grades. Furthermore, most of the previous studies only reported the differences between low- (grade I) and intermediate-/high-grade (grade II/III) meningiomas on ADC images. The differences between grade II and III have rarely been investigated using MRI findings; therefore, more information to find an appropriate model for distinguishing grades II and III on MRI images is needed. Owing to this, the purpose of the present study was to use the volumetric histogram parameters of the ADC map and the conventional T1- and T2-weighted images for differentiating high-, intermediate-, and low-grade meningiomas, as well as analyzing the possibility of using several parameters for predicting meningioma tumor grade.

Methods

This retrospective study was carried out following the relevant guidelines and regulations, and the methods used in this study were approved by the National Ethics Committee. The MRI images of patients were used in this study without any intervention in the diagnostic or treatment procedures. In addition, informed consent was waived because of the retrospective nature of the study.

Patients

Overall, preoperative MRI images of 45 patients with the diagnosis of meningioma tumors at different grades (9 patients with grade III, 16 patients with grade II, and 20 patients with grade I tumors) were used in this study. The participants consisted of 15 men and 30 women with a mean age of 55.6 ± 9.1 years, ranging from 34 to 75.

The images of the patients were collected from the database of the Imaging Department, Tajrish Hospital (one of the biggest hospitals in Tehran, Iran). The imaging procedures of all the images used in the present study were performed during 2019 and 2020. Tumor grading according to the WHO classification [11] was obtained from the patients' health documents archived in the imaging department.

The patients did not have any history of brain surgery and the MRI images were taken before the biopsy procedure. In addition, participants with a history of chemotherapy or radiotherapy were excluded from this study. Notably, there were several inclusion criteria for the patients' MRI images; the assessed tumors had to be primarily bigger than 10 mm in size (in the smallest dimension), and the data related to tumor grading had to be available based on WHO classification [11]. Furthermore, MRI images had to contain transversal T1 (pre- and post-contrast), T2, T2-FLAIR-weighted images along with ADC maps data.

MRI protocols

Imaging procedures were performed using 1.5T scanners (Siemens MAGNETOM Avanto, Siemens Healthcare, Germany) using a head coil. In this study, the following sequences were analyzed: axial T1-weighted (pre- and post-contrast images), fast spin-echo sequence (TR 400 ms, TE 14 ms, flip angle 90°, 4-mm slice thickness, and 280-mm field of view), axial T2-weighted (TR 2820 ms, TE 95 ms, flip angle 90°, 4-mm slice thickness, and 280 mm field of view), and axial T2- FLAIR (TR 8000 ms, TE 125 ms, flip angle 90°, inversion time 2000, 4-mm slice thickness, and 280-mm field of view). The ADC images were acquired by applying diffusion gradients in three independent directions. All images were taken by three gradient b-values of 0, 500, and 1000 mm^2/s respectively. DICOM (digital imaging and communication

on medicine) software (DicomWorks v1.3.5 2000, 2002; License: Freeware Free; Publishers: Phillippe Puech and Loic Bousse) was used to obtain the ADC values (ADC map) in different regions of diffusion-weighted MRI images.

Analyzing the image

All the MR images and ADC maps were saved in DICOM format for better prevention of image information loss. The images were imported to Ray station treatment planning software (Version 8.A, Raysearch Laboratories, Sweden) and the tumor region (the whole lesion based on the tumor boundaries), as well as normal brain tissue, were then contoured in the post-contrast T1-weighted images (slice by slice) and subsequently mapped (copied in the same region) on the other image sequences. The treatment planning software reconstructed the volume by connecting the contoured ROIs in all the MRI slices. The details of volume reconstruction using ROIs and contoured in series of two-dimensional images with known slice thickness were explained in a previous report [12]. Two independent radiation oncologists contoured the ROIs of tumor and brain, and an experienced radiation oncologist (with more than 20 years of experience) reviewed the contours of tumors in all the patients to ensure that the correct tumor region was selected.

The MR images alongside the related structures (in DICOM format) were imported to the CERR (Computational Environment in Radiotherapy Research) [13], a MATLAB-based application (MATLAB Ver.2019b, MathWorks company, MA, USA). In summary, CERR allowed us to use DICOM structures delineated in the treatment planning system on MR images and obtain the three-dimensional intensity histogram in each of the image sequences. After obtaining the histogram of the tumor and normal brain tissue for every image, the following parameters were calculated: mean; maximum value; minimum value; median; mode; and 10th, 25th, 50th, 75th, and 90th percentiles as well as kurtosis and skewness.

Statistical analysis

The parameters derived from three-dimensional histograms from each of the image sets were compared between different tumor grade groups utilizing the non-parametric statistical Kruskal-Wallis test. Furthermore, the multi-parametric linear regression analyses were used to find a model from selected histogram parameters having higher predictive value (i.e., having lower P values) for differentiating the meningioma grades in different MRI image series. In addition, Spearman's correlation was performed to find the correlation coefficients between the histogram parameters with significant differences (P value < 0.05) using all the patients' data (without considering the tumor grade) in different MRI image series. The receiver operating characteristic (ROC) curve was used to evaluate the diagnostic ability of the histogram parameter values to differentiate between high-, intermediate-, and low-grade meningioma tumors. The cutoff value was chosen to maximize the Youden index. Furthermore, sensitivity and specificity (at cutoff points), and also the AUC (area under the curve) values, were calculated using the obtained ROC curves. The level of statistical significance was set at $P < 0.05$, and all the statistical tests were performed using SPSS software package, V18 (SPSS Inc., Chicago, USA).

Results

Some examples of ADC volumetric histograms and MR images obtained from meningioma tumors at different grades (one patient for each grade) are shown in Fig. 1. The histogram changes with tumor grade are obvious in this figure, in such a way that, histogram mode, median, and mean values of ADC images differ significantly at different tumor grades ($P < 0.03$). Furthermore, the 75th and 90th percentiles showed significantly lower values in higher tumor grades.

The tumor volumetric histogram example on T1-post-contrast images are presented in Fig. 2 (one patient for each grade) for different tumor grades. In T2-FLAIR images, the histogram mode (maximum intensity) showed significant differences between grade I and grade II/III ($P < 0.03$). None of the tumor histogram parameters in pre-contrast T1-weighted and T2-weighted images showed any significant differences between different meningioma tumor grades ($P > 0.2$), except in the range (maximum−minimum) in T2WI ($P < 0.04$).

The histogram ranges differed significantly between three tumor grades on T1-WI post-contrast, T2-WI, T2-FLAIR, and ADC images. The standard deviation and variance were significantly different between the groups at ADC, T2-FLAIR, and T1-WI post-contrast. A significant difference was also observed between tumor grades for the modal intensity, mean value, 25th, 50th, and 90th percentiles in post-contrast T1-WI, meaning that all the parameters had a direct relationship with tumor grades.

Tumor histogram kurtosis of post-contrast T1-WI and T2-FLAIR images showed significant differences among grade I compared to grades II and III meningiomas ($P < 0.03$); however, no differences were found between grades II and III regarding the kurtosis in these images. Furthermore, skewness was not a predictive histogram parameter in our study, due to the fact there were that no statistically significant differences relating to different tumor grades in all the assessed MRI image series. The obtained histogram parameters' values with reported P

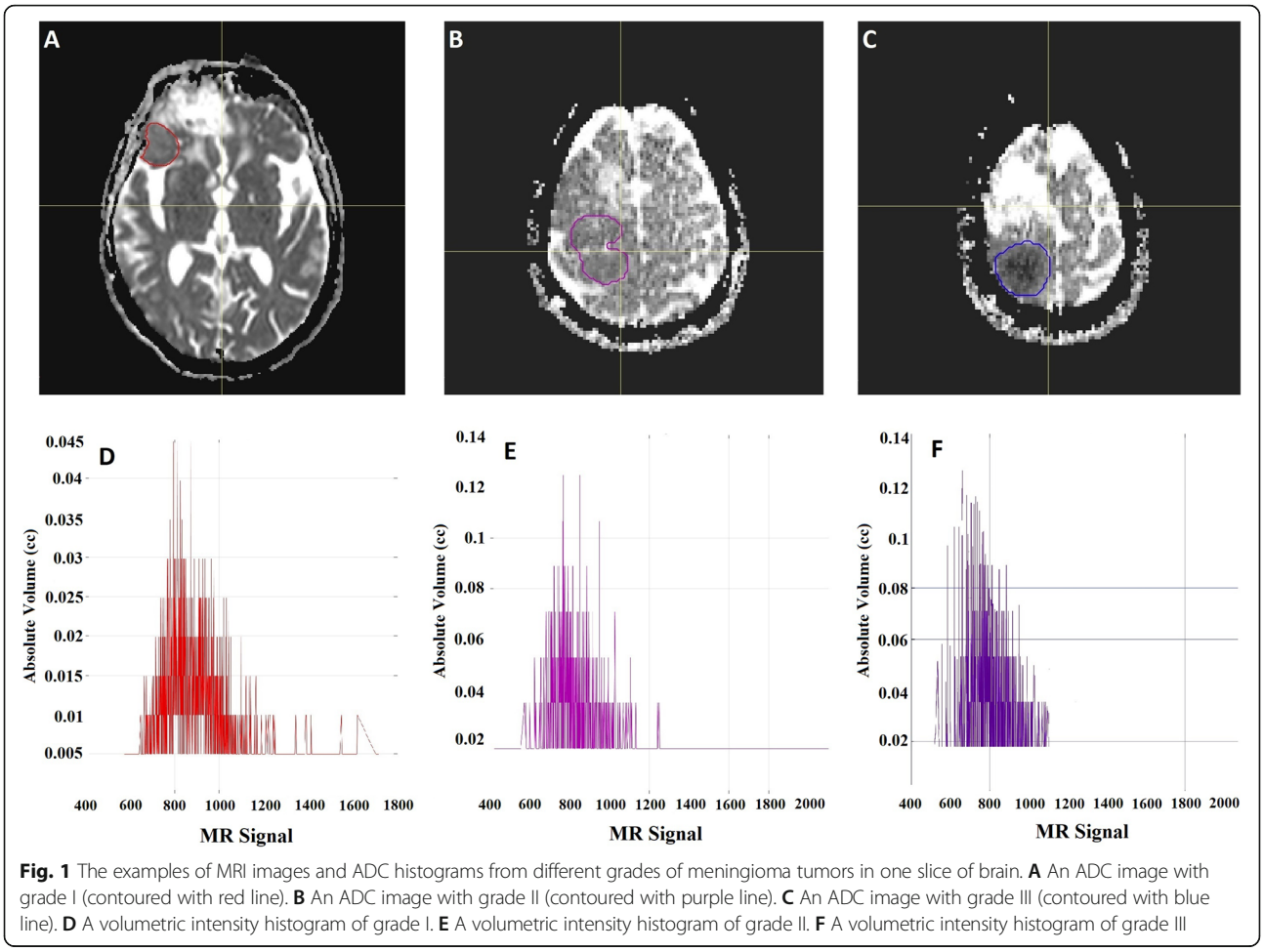

Fig. 1 The examples of MRI images and ADC histograms from different grades of meningioma tumors in one slice of brain. **A** An ADC image with grade I (contoured with red line). **B** An ADC image with grade II (contoured with purple line). **C** An ADC image with grade III (contoured with blue line). **D** A volumetric intensity histogram of grade I. **E** A volumetric intensity histogram of grade II. **F** A volumetric intensity histogram of grade III

values between different tumor grades are presented in Table 1.

The correlation coefficient of histogram parameters with high predictive value (i.e., low P values) is presented as matrix heat maps in Fig. 3.

For multi-parametric linear regression analysis 2 out of 4 parameters on T2-FLAIR, 4 out of 8 parameters on post-contrast T1-WI, and 4 out of 7 on ADC images, were selected, which had high predictive value to establish models (with P values lower than 0.02).

The optimal multi-parametric regression models of T1-WI post-contrast, T2-FLAIR, and ADC images were determined as follows:

$$\begin{aligned} &f(\text{contrasted T1–WI}) = 0.01 \\ &\times[5.22 + 7.64\text{e}{-3} \times \text{mode} + 3.18\text{e}{-3} \times \text{mean} - 1.10\text{e}{-4} \times \text{median} - 8.31\text{e}{-5} \times 90\text{th}] \end{aligned} \tag{1}$$

$$f(\text{T2–FLAIR}) = 0.01 \times [5.41 + 2.22\text{e}{-3} \times \text{mode} + 2.03\text{e}{-2} \times \text{SD}] \tag{2}$$

$$\begin{aligned} &f(\text{ADC}) = 0.01 \\ &\times[3.54 + 2.28\text{e}{-2} \times \text{mode} + 1.11\text{e}{-4} \times \text{mean} + 5.11\text{e}{-5} \times \text{median} + 1.23\text{e}{-4} \times 90\text{th}] \end{aligned} \tag{3}$$

In Fig. 4, the ROC curves including the model cutoff values, sensitivity, specificity, and AUC values are shown for differentiating the tumor grades (I from II; and II from III).

The volumetric histogram parameters of ADC images showed higher predictive power having cutoff values of 0.212 (sensitivity = 79.6%, specificity = 84.3%, and AUC = 0.852) and 0.180 (sensitivity = 70.9%, specificity = 80.8%, and AUC = 0.833) for differentiating the grade I from II, and grade II from III, respectively.

Discussion

The present study showed that analysis of volumetric histogram parameters derived from ADC, post-contrast T1WI, and T2-FLAIR images in meningioma can reflect relevant tumor grading features. In a study by Li et al. [14], volumetric histograms of conventional MRI (T1- and T2-weighted images) were analyzed, and it was

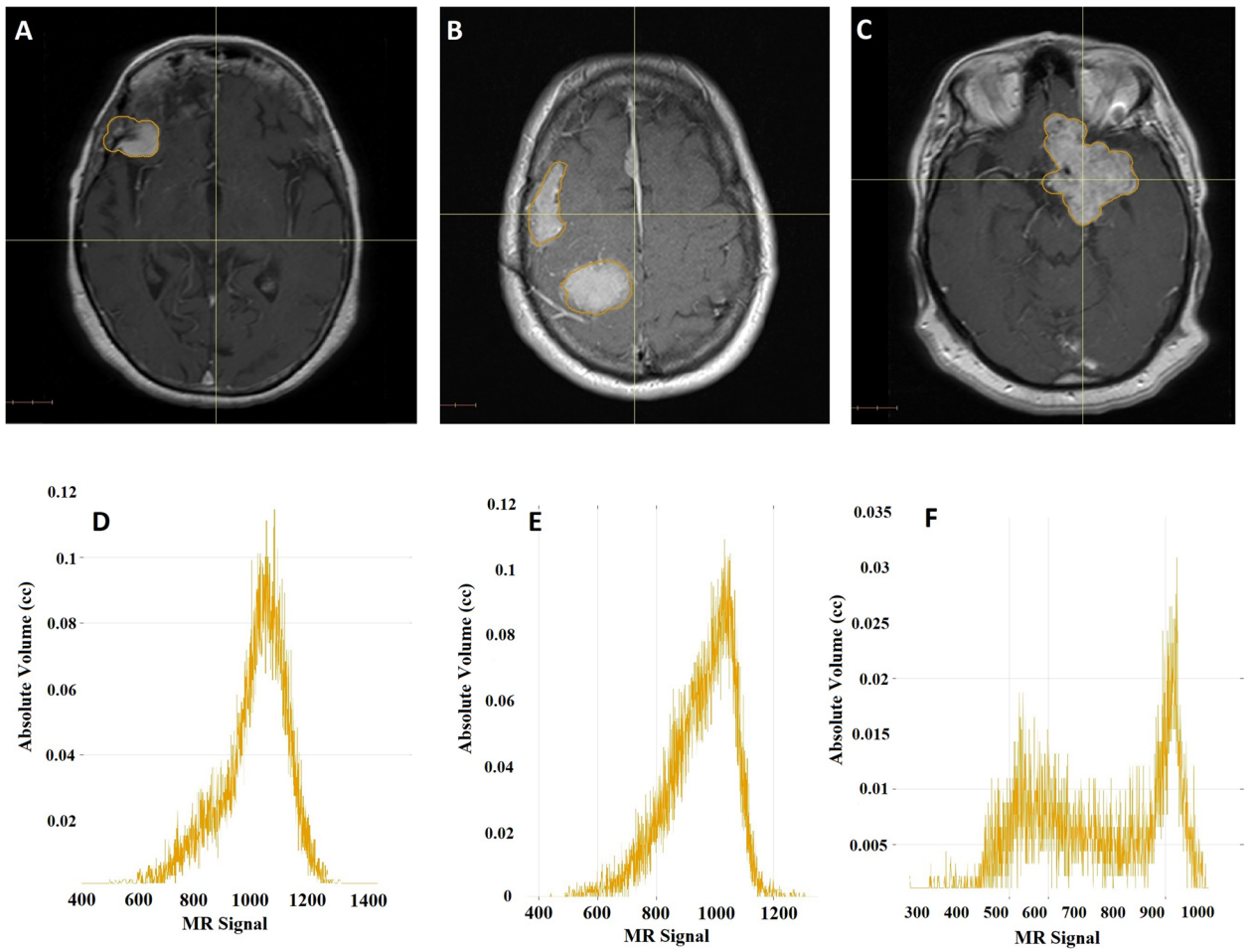

Fig. 2 The examples of post-contrast MRI images and T1-WI histograms obtained from different grades of meningioma tumors in one slice of brain. **A** T1-WI image with grade I (contoured with orange line). **B** T1-WI image with grade II (contoured with orange line). **C** T1-WI image with grade III (contoured with blue line). **D** A volumetric intensity histogram of grade I. **E** A volumetric intensity histogram of grade II. **F** A volumetric intensity histogram of grade III

reported that the kurtosis, standard deviation, the maximum intensity of T2WI, skewness, mean deviation, minimum intensity, mean value, 5th percentile, 10th percentile, 25th percentile, 50th percentile, 75th percentile, and 90th percentile of contrasted T1WI were predictive parameters in distinguishing high-grade meningioma (grades II/III) from low-grade. There are some differences in derived parameters between our findings compared to this study. For instance, we did not find any parameter in T2WI as a predictive tool for distinguishing different grades of meningioma tumors. This may be related to finding the parameters that are able to differentiate all the three meningioma grades in our study, instead of differentiating just high and low-grade meningioma.

In a study by Meyer et al. [10], skewness derived from pre-contrast T1WI correlated with Ki-67 index. Furthermore, entropy derived from pre-contrast T1WI correlated with the average of nucleic area. It was shown that several parameters from post-contrast T1WI correlated with nucleic count: maximum signal intensity, P75, and 90th percentile as well as standard deviation. For the T2-FLAIR sequence, maximum signal intensity correlates with the nucleic count. They concluded that volumetric histogram parameters of conventional MRI sequences can reflect different histopathological features in primary central nervous system lymphoma. Although meningioma and lymphoma are different tumors, we also found that maximum intensity and 90th percentile in post-contrast T1-WI and maximum intensity in T2-FLAIR images were the histogram parameters showing differences between different meningioma grades. In addition, Meyer et al. [15] in another investigation, assessed the multiple associations between volumetric histogram parameters derived from T1WI and T2WI image series, and also clinically relevant histopathological features were found in head and neck squamous

Table 1 Mean ± standard deviation of histogram parameters with resulted P values between different tumor grades obtained from ADC, post-contrast T1WI, and T2-FLAIR images

Parameter	Grade I	Grade II	Grade III	P value
ADC ($\times 10^{-6}$ mm^2/s)				
Mean intensity	895.2 ± 9.3	678.6 ± 5.9	605.1 ± 8.5	< 0.01
Modal intensity	863.5 ± 10.6	659.4 ± 6.6	588.7 ± 5.8	< 0.01
Median intensity	910.3 ± 12.7	697.8 ± 7.4	613.0 ± 13.2	0.01
Maximum value	1233.2 ± 114.5	1205 ± 143.4	1162.7 ± 157.6	0.21
Minimum value	582 ± 88.5	535 ± 76.9	518 ± 98.6	0.15
10th percentile	645.6 ± 51.4	638.9 ± 44.6	622.2 ± 58.7	0.09
25th percentile	736.9 ± 55.4	725.5 ± 41.15	704.4 ± 54.3	0.11
75th percentile	1094.7 ± 33.6	1003.6 ± 37.5	927.6 ± 45.8	0.04
90th percentile	1148.8 ± 39.8	1044.5 ± 41.5	986.6 ± 46.0	0.02
Kurtosis	3.8 ± 0.6	3.5 ± 0.8	3.7 ± 1.2	0.08
Skewness	0.06 ± 0.11	0.07 ± 0.16	0.03 ± 0.18	0.24
SD	64.5 ± 13.3	56.6 ± 11.2	48.8 ± 13.7	0.02
T1WI-post-contrast				
Mean intensity	1116.3 ± 84.5	1025.1 ± 79.6	818.6 ± 95.6	< 0.01
Modal intensity	1195.7 ± 88.9	1134.2 ± 85.1	925.7 ± 99.3	< 0.01
Median intensity	1044.8 ± 76.7	984.3 ± 78.1	776.3 ± 88.8	< 0.01
Maximum value	1343.8 ± 174.7	1296.3 ± 152.0	1158.7 ± 181.6	0.31
Minimum value	258.7 ± 94.6	225.6 ± 93.5	181.8 ± 76.6	0.24
10th percentile	512.9 ± 64.2	473.8 ± 58.7	426.3 ± 76.3	0.18
25th percentile	856.6 ± 58.2	731.3 ± 55.9	628.5 ± 61.8	0.04
75th percentile	1224.7 ± 90.4	1191.5 ± 87.2	989.6 ± 92.5	0.07
90th percentile	1296.8 ± 61.2	1238.5 ± 60.6	1078.9 ± 78.1	0.02
Kurtosis	3.9 ± 1.3	4.0 ± 1.2	5.3 ± 1.4	0.03
Skewness	− 0.36 ± 0.21	− 0.31 ± 0.24	− 0.19 ± 0.38	0.49
SD	128.7 ± 22.1	106.0 ± 23.6	95.4 ± 25.5	0.03
T2WI-FLAIR				
Mean intensity	567.9 ± 67.4	523.6 ± 78.3	505.4 ± 79.9	0.09
Modal intensity	753.2 ± 54.6	678.4 ± 55.1	615.4 ± 58.0	0.01
Median intensity	659.2 ± 60.5	615.3 ± 66.9	578.3 ± 75.4	0.18
Maximum value	875.5 ± 82.3	794.8 ± 81.7	742.2 ± 75.2	0.16
Minimum value	189.5 ± 67.4	157.0 ± 65.2	201.2 ± 73.5	0.47
10th percentile	331.2 ± 58.2	302.6 ± 48.6	291.4 ± 52.3	0.28
25th percentile	385.5 ± 74.8	347.6 ± 66.7	321.2 ± 72.5	0.32
75th percentile	724.3 ± 86.9	688.3 ± 85.4	645.0 ± 91.6	0.21
90th percentile	814.6 ± 81.5	734.7 ± 77.9	692.2 ± 71.8	0.15
Kurtosis	4.1 ± 1.5	4.3 ± 0.9	5.8 ± 1.2	0.03
Skewness	− 0.43 ± 0.31	− 0.45 ± 0.28	− 0.31 ± 0.29	0.54
SD	58.2 ± 8.8	44.6 ± 6.4	36.3 ± 9.1	0.02

cell carcinoma (HNSCC). They have reported that volumetric histogram parameters can be used as surrogate markers for tumor cellularity, proliferation, and vascularization in HNSCC.

Although most of the previous studies have reported the relationship between the histogram parameters and brain tumor behavior, several studies are presenting the same results for tumors located outside

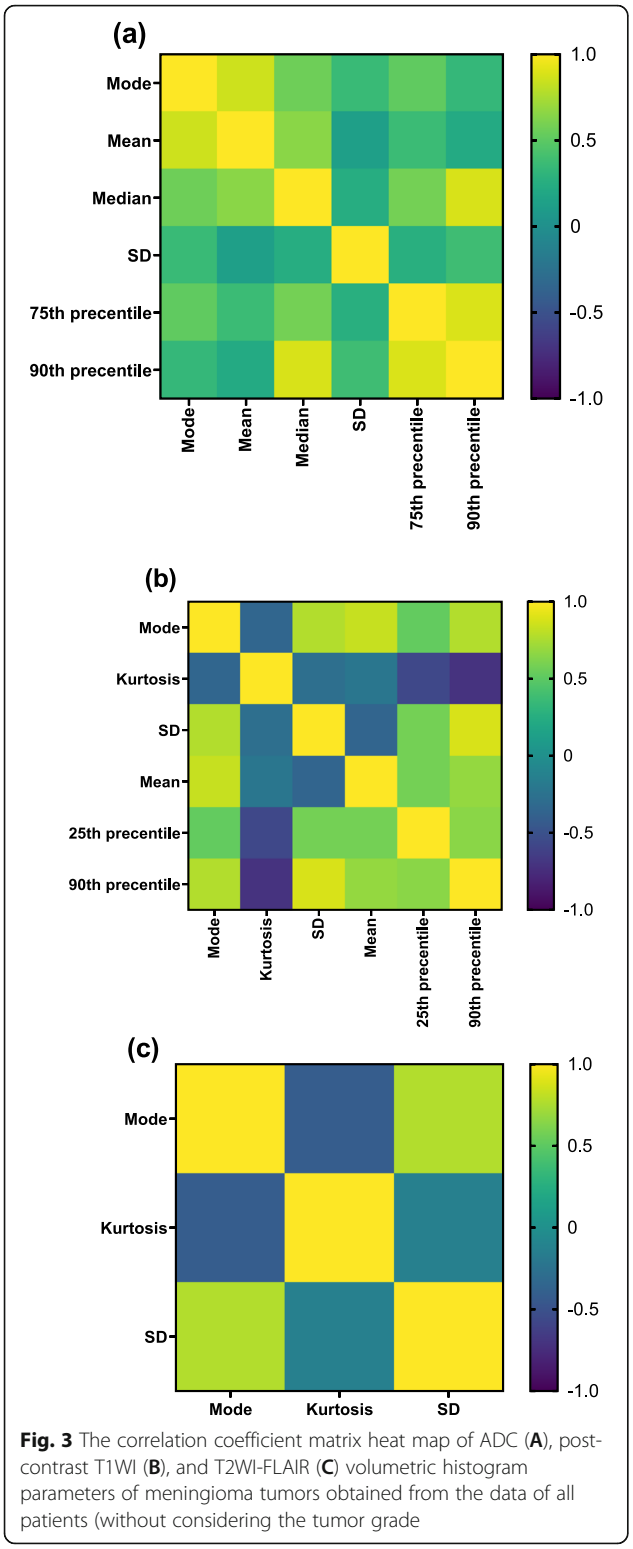

Fig. 3 The correlation coefficient matrix heat map of ADC (**A**), post-contrast T1WI (**B**), and T2WI-FLAIR (**C**) volumetric histogram parameters of meningioma tumors obtained from the data of all patients (without considering the tumor grade

the brain [9, 16–18]. For instance, it has been reported that histogram analysis parameters of T1-WI and T2-WI reflect HER2 status and EGFR expression in cervical cancer [19].

Conclusion

The signal intensity in FLAIR sequences is largely influenced by both T1 and T2 relaxation time; there

is a close relationship between the signal intensity of brain tumors on T2-weighted images and the degree of contrast enhancement on FLAIR sequences. When tumors have higher signal intensity than normal cortex on T2-weighted images, additional postcontrast FLAIR imaging may improve their depiction.

Several studies have reported that volumetric ADC histogram analysis could differentiate high and low-grade meningioma and they suggested that ADC histogram analysis is an accurate tool to predict tumor behavior in the brain and other sites [14, 20]. In a study by Nagar et al. [5], grades II and III meningioma were statistically and significantly lower in several ADC values (median, mean, mode, 10th percentile, and 90th percentile) in comparison to grade I tumors, which is in line with the current work. Moreover, in their study, two parameters, namely median and 10th percentile were more sensitive in comparison to other ADC values and this can distinguish grade I meningioma from grade II/III tumors with higher sensitivity. In contrast, we found that the mean, mode, 75th percentile and 90th percentile values had higher sensitivity in showing different meningioma grades because analyzing the ADC volumetric histograms was more accurate for the detection of tumor grade in comparison to widely used mean and/or minimal ADC values in selective ROIs in just one slice of MRI images [21–23]. This is due to the fact that analyzing the volumetric histogram yields information about the whole tumor volume, whereas analyzing the histogram in a two-dimensional ROI has just the information of small parts of the tumor. For example, it was shown that in cervical cancer, volumetric ADC histogram analysis can predict lymph node metastases [10]. Overall, previous reports have suggested that ADC histogram analysis is a sensitive instrument to predict tumor behavior in the brain and other sites. Other MRI images (like conventional T1WI and T2WI) have rarely been investigated for finding a relationship between the tumor behavior/grade with volumetric histogram parameters of the tumor.

Findings from our study showed that ADC images are more sensitive to distinguish different meningioma grades compared to other conventional MRI images like T1- and T2-weighted images. However, ROC analysis showed that post-contrast T1WI is also an appropriate grade-differentiating tool for meningioma tumors. No

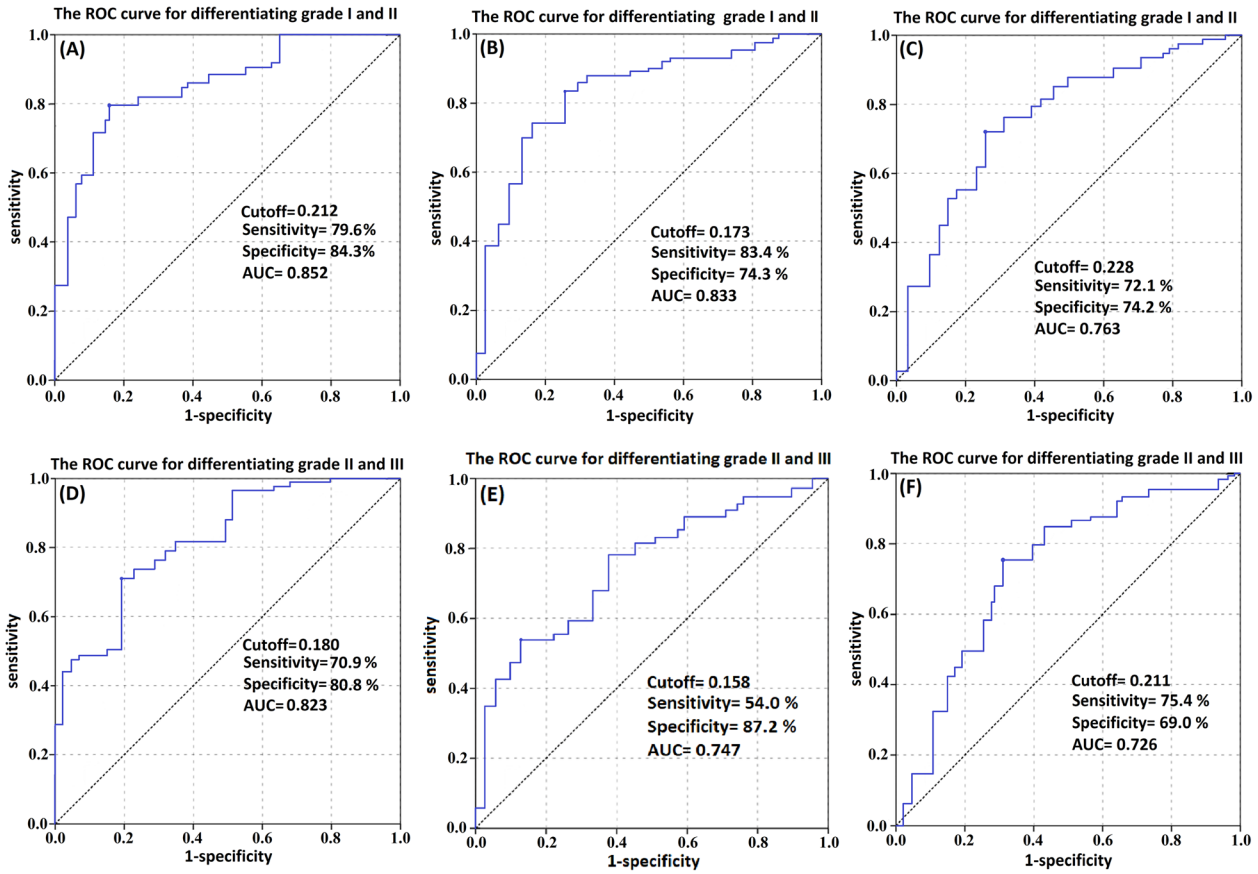

Fig. 4 ROC curves including the model cutoff values, sensitivity, specificity, and AUC for differentiating the tumor grades (I from II; and II from III). **A** ROC curve obtained from the model fitted to ADC histogram parameters for differentiating grade I and II meningioma tumors. **B** ROC curve obtained from the model fitted to post-contrast T1WI histogram parameters for differentiating grades I and II meningioma tumors. **C** ROC curve obtained from the model fitted to T2WI-FLAIR histogram parameters for differentiating grades I and II meningioma tumors. **D** ROC curve obtained from the model fitted to ADC histogram parameters for differentiating grades II and III meningioma tumors. **E** ROC curve obtained from the model fitted to post-contrast T1WI histogram parameters for differentiating grades II and III meningioma tumors. **F** ROC curve obtained from the model fitted to T2WI-FLAIR histogram parameters for differentiating grades II and III meningioma tumors

studies have compared the volumetric histogram parameters of different conventional MRI image sequences and ADC performance for differentiation of meningioma grades.

In the current study, higher heterogeneity was observed in higher meningioma grades compared to low-grade ones, especially in post-contrast T1-weighted images. This phenomenon may be related to the presence of internal cystic degeneration, necrosis, and hemorrhage in higher meningioma grades [8, 24–26]. It was reported that skewness and kurtosis represent the distribution of histogram curves and can indicate the tumor heterogeneity. Therefore, these parameters can predict the malignancy degree of the tumor [27]. However, we found that the skewness does not have any predictive value to show the meningioma tumor grade. There is some contradictory information about kurtosis and skewness of meningioma tumors at different grades. For example, in a study by Wang et al. [28], higher kurtosis and skewness were reported in atypical or malignant meningiomas compared to low-grade meningiomas. In contrast, higher kurtosis and skewness values in low-grade meningiomas were reported by Li et al. [14], which is in agreement with our findings of the kurtosis. The discrepancy existing between the findings may have resulted from angiomatous meningioma, which is a subtype of grade I meningiomas but resembles high-grade aggressive meningiomas [29, 30]. In post-contrast images, usually, meningiomas are observed with high enhancement due to significantly high blood supply especially in angiomatous meningiomas. This type of meningioma has a large number of blood vessels occupying more than 50% of the tumor volume and the blood supply usually is higher than the malignant tumors [31].

One of the limitations of our study was the small number of patients in the grade III group. Furthermore,

other MRI image sequences and measurements like T1-FLAIR, proton density, and T2*-weighted images along with the MR-spectroscopy measurements could be investigated to explore their ability for differentiating meningioma grades in future research.

Conclusions

Analyzing the parameters obtained from tumor volumetric histograms in some of the conventional MRI series (i.e., post-contrast T1 and T2-FLAIR images) along with the ADC images can be a good predictive model for the assessment of meningioma grading. The multiparametric linear regression model obtained from ADC (with sensitivity > 70% and specificity > 80%) and contrasted T1WI histogram parameters showed promising assessments for meningioma grading. Mean, mode, median, and 90th percentile values in these two image series are the most powerful predictors for meningioma tumor grading.

Abbreviations

ADC: Apparent Diffusion coefficient; MRI: Magnetic resonance imaging; CNS: Central nervous system; WHO: World health organization; DWI: Diffusion-weighted imaging; ROC: Receiver operating characteristic; AUC: Area under the curve; ROI: Region of interest

Acknowledgements

The patients' imaging was acquisitioned from Department of Radiology, Imam Khomeini Hospital (Tehran, Iran). Therefore, the authors express their sincere appreciation to the staff members of the above center.

Authors' contributions

M. H. B.: all steps of the study from conception to manuscript drafting and approval of the final version. M. F.: conception and design of the study, critical revision of the manuscript, analyzing, and interpretation of data. S. R. Y.: acquisition of data, critical revision of the manuscript, and approval of the final version. A. T. A.: critical revision of the manuscript, analyzing, and interpretation of data. G. A.: analyzing and interpretation of data and critical revision of the manuscript. K. S.: conception and design of the study, analyzing and interpretation of data, and critical revision of the manuscript. S. M. M.: analyzing and interpretation of data, critical revision of the manuscript, and approval of the final version. R. A. F.: design of the study, analyzing and interpretation of data, critical revision of the manuscript, and approval of the final version. All authors have read and approved the manuscript.

Funding

None.

Availability of data and materials

The datasets used and/or analyzed during the current study are available from the corresponding author on reasonable request.

Declarations

Ethics approval and consent to participate

Our study was approved by Shahid Sadoughi University of Medical Sciences (Yazd, Iran) with the registration number of "IR.SSU.MEDICINE.REC.1395.297".

Consent for publication

Not applicable.

Competing interests

The authors declare that they have no competing interests.

Author details

[1]Department of Medical Physics, Isfahan University of Medical Sciences, Isfahan, Iran. [2]Student of Medical Physics, Department of Medical Physics, Tarbiat Modares University, Tehran, Iran. [3]Department of Medical Physics, School of Medicine, Zahedan University of Medical Sciences, Zahedan, Iran. [4]Department of Medical Physics, School of Medicine, Shahid Sadoughi University of Medical Sciences, Yazd, Iran. [5]Department of Medical Physics, Tehran University of Medical Sciences, Tehran, Iran. [6]Department of Radiology Technology, Faculty of Paramedical Sciences, Babol University of Medical Science, Babol, Iran. [7]Department of Medical Physics, Faculty of Medicine, Mashhad University of Medical Sciences, Mashhad, Iran. [8]Cellular and Molecular Research Center, Yasuj University of Medical Sciences, Yasuj, Iran.

Received: 26 April 2021 Accepted: 26 June 2021
Published online: 07 July 2021

References

1. Louis DN, Perry A, Reifenberger G, Von Deimling A, Figarella-Branger D, Cavenee WK et al (2016) The 2016 World Health Organization classification of tumors of the central nervous system: a summary. Acta Neuropathol (Berl) 131(6):803–820. https://doi.org/10.1007/s00401-016-1545-1
2. Saloner D, Uzelac A, Hetts S, Martin A, Dillon W (2010) Modern meningioma imaging techniques. J Neuro-Oncol 99(3):333–340. https://doi.org/10.1007/s11060-010-0367-6
3. Surov A, Ginat DT, Lim T, Cabada T, Baskan O, Schob S, Meyer HJ, Gihr GA, Horvath-Rizea D, Hamerla G, Hoffmann KT, Wienke A (2018) Histogram analysis parameters apparent diffusion coefficient for distinguishing high and low-grade meningiomas: a multicenter study. Transl Oncol 11(5):1074–1079. https://doi.org/10.1016/j.tranon.2018.06.010
4. Hakyemez B, Yıldırım N, Gokalp G, Erdogan C, Parlak M (2006) The contribution of diffusion-weighted MR imaging to distinguishing typical from atypical meningiomas. Neuroradiology. 48(8):513–520. https://doi.org/10.1007/s00234-006-0094-z
5. Nagar VA, Ye JR, Ng WH, Chan YH, Hui F, Lee CK, Lim CCT (2008) Diffusion-weighted MR imaging: diagnosing atypical or malignant meningiomas and detecting tumor dedifferentiation. Am J Neuroradiol 29(6):1147–1152. https://doi.org/10.3174/ajnr.A0996
6. Surov A, Ginat DT, Sanverdi E, Lim CT, Hakyemez B, Yogi A et al (2016) Use of diffusion weighted imaging in differentiating between maligant and benign meningiomas. A multicenter analysis. World Neurosurg 88:598–602. https://doi.org/10.1016/j.wneu.2015.10.049
7. Surov A, Gottschling S, Mawrin C, Prell J, Spielmann RP, Wienke A, Fiedler E (2015) Diffusion-weighted imaging in meningioma: prediction of tumor grade and association with histopathological parameters. Transl Oncol 8(6):517–523. https://doi.org/10.1016/j.tranon.2015.11.012
8. Just N (2014) Improving tumour heterogeneity MRI assessment with histograms. Br J Cancer 111(12):2205–2213. https://doi.org/10.1038/bjc.2014.512
9. Meyer HJ, Leifels L, Schob S, Garnov N, Surov A (2018) Histogram analysis parameters identify multiple associations between DWI and DCE MRI in head and neck squamous cell carcinoma. Magn Reson Imaging 45:72–77. https://doi.org/10.1016/j.mri.2017.09.015
10. Meyer H-J, Schob S, Münch B, Frydrychowicz C, Garnov N, Quäschling U, Hoffmann KT, Surov A (2018) Histogram analysis of T1-weighted, T2-weighted, and postcontrast T1-weighted images in primary CNS lymphoma: correlations with histopathological findings—a preliminary study. Mol Imaging Biol 20(2):318–323. https://doi.org/10.1007/s11307-017-1115-5
11. Whittle IR, Smith C, Navoo P, Collie D (2004) Meningiomas. Lancet 363(9420):1535–1543. https://doi.org/10.1016/S0140-6736(04)16153-9
12. Thornton AF Jr, Sandler HM, Ten Haken RK, McShan DL, Fraass BA, LaVigne ML, Yanks BR (1992) The clinical utility of magnetic resonance imaging in 3-dimensional treatment planning of brain neoplasms. Int J Radiat Oncol Biol Phys 24(4):767–775. https://doi.org/10.1016/0360-3016(92)90727-Y
13. Deasy JO, Blanco AI, Clark VH (2003) CERR: a computational environment for radiotherapy research. Med Phys 30(5):979–985. https://doi.org/10.1118/1.1568978
14. Li X, Miao Y, Han L, Dong J, Guo Y, Shang Y, Xie L, Song Q, Liu A (2019) Meningioma grading using conventional MRI histogram analysis based on 3D tumor measurement. Eur J Radiol 110:45–53. https://doi.org/10.1016/j.ejrad.2018.11.016

15. Meyer HJ, Leifels L, Hamerla G, Höhn AK, Surov A (2019) Histogram analysis parameters derived from conventional T1-and T2-weighted images can predict different histopathological features including expression of Ki67, EGFR, VEGF, HIF-1α, and p53 and cell count in head and neck squamous cell carcinoma. Mol Imaging Biol 21(4):740–746. https://doi.org/10.1007/s11307-018-1283-y
16. Woo S, Cho JY, Kim SY, Kim SH (2014) Histogram analysis of apparent diffusion coefficient map of diffusion-weighted MRI in endometrial cancer: a preliminary correlation study with histological grade. Acta Radiol 55(10):1270–1277. https://doi.org/10.1177/0284185113514967
17. Waldenberg C, Hebelka H, Brisby H, Lagerstrand KM (2018) MRI histogram analysis enables objective and continuous classification of intervertebral disc degeneration. Eur Spine J 27(5):1042–1048. https://doi.org/10.1007/s00586-017-5264-7
18. Barrett T, Lawrence EM, Priest AN, Warren AY, Gnanapragasam VJ, Gallagher FA, Sala E (2019) Repeatability of diffusion-weighted MRI of the prostate using whole lesion ADC values, skew and histogram analysis. Eur J Radiol 110:22–29. https://doi.org/10.1016/j.ejrad.2018.11.014
19. Meyer H-J, Hamerla G, Höhn AK, Surov A (2019) Whole lesion histogram analysis derived from morphological MRI sequences might be able to predict EGFR-and Her2-expression in cervical cancer. Acad Radiol 26(8):e208–e215. https://doi.org/10.1016/j.acra.2018.09.008
20. Kang Y, Choi SH, Kim Y-J, Kim KG, Sohn C-H, Kim J-H, Yun TJ, Chang KH (2011) Gliomas: histogram analysis of apparent diffusion coefficient maps with standard-or high-b-value diffusion-weighted MR imaging—correlation with tumor grade. Radiology. 261(3):882–890. https://doi.org/10.1148/radiol.11110686
21. Schob S, Meyer HJ, Pazaitis N, Schramm D, Bremicker K, Exner M, Höhn AK, Garnov N, Surov A (2017) ADC histogram analysis of cervical cancer aids detecting lymphatic metastases—a preliminary study. Mol Imaging Biol 19(6):953–962. https://doi.org/10.1007/s11307-017-1073-y
22. Schob S, Meyer HJ, Dieckow J, Pervinder B, Pazaitis N, Höhn AK, Garnov N, Horvath-Rizea D, Hoffmann KT, Surov A (2017) Histogram analysis of diffusion weighted imaging at 3T is useful for prediction of lymphatic metastatic spread, proliferative activity, and cellularity in thyroid cancer. Int J Mol Sci 18(4):821. https://doi.org/10.3390/ijms18040821
23. Meyer HJ, Höhn A, Surov A (2018) Histogram analysis of ADC in rectal cancer: associations with different histopathological findings including expression of EGFR, Hif1-alpha, VEGF, p53, PD1, and KI 67. A preliminary study. Oncotarget 9(26):18510
24. Ahn SJ, Choi SH, Kim Y-J, Kim KG, Sohn C-H, Han MH, Chang KH, Min HS (2012) Histogram analysis of apparent diffusion coefficient map of standard and high B-value diffusion MR imaging in head and neck squamous cell carcinoma: a correlation study with histological grade. Acad Radiol 19(10):1233–1240. https://doi.org/10.1016/j.acra.2012.04.019
25. Ryu YJ, Choi SH, Park SJ, Yun TJ, Kim J-H, Sohn C-H (2014) Glioma: application of whole-tumor texture analysis of diffusion-weighted imaging for the evaluation of tumor heterogeneity. PLoS One 9(9):e108335. https://doi.org/10.1371/journal.pone.0108335
26. Skogen K, Schulz A, Dormagen JB, Ganeshan B, Helseth E, Server A (2016) Diagnostic performance of texture analysis on MRI in grading cerebral gliomas. Eur J Radiol 85(4):824–829. https://doi.org/10.1016/j.ejrad.2016.01.013
27. Baek HJ, Kim HS, Kim N, Choi YJ, Kim YJ (2012) Percent change of perfusion skewness and kurtosis: a potential imaging biomarker for early treatment response in patients with newly diagnosed glioblastomas. Radiology. 264(3):834–843. https://doi.org/10.1148/radiol.12112120
28. Wang S, Kim S, Zhang Y, Wang L, Lee EB, Syre P, Poptani H, Melhem ER, Lee JYK (2012) Determination of grade and subtype of meningiomas by using histogram analysis of diffusion-tensor imaging metrics. Radiology. 262(2):584–592. https://doi.org/10.1148/radiol.11110576
29. Azizyan A, Eboli P, Drazin D, Mirocha J, Maya MM, Bannykh S (2014) Differentiation of benign angiomatous and microcystic meningiomas with extensive peritumoral edema from high grade meningiomas with aid of diffusion weighted MRI. Biomed Res Int 2014:1–7. https://doi.org/10.1155/2014/650939
30. Liu Z, Wang C, Wang H, Wang Y, Li JY, Liu Y (2013) Clinical characteristics and treatment of angiomatous meningiomas: a report of 27 cases. Int J Clin Exp Pathol 6(4):695–702
31. Zakhari N, Torres C, Castillo M, Nguyen TB (2017) Uncommon cranial meningioma: key imaging features on conventional and advanced imaging. Clin Neuroradiol 27(2):135–144. https://doi.org/10.1007/s00062-017-0583-y

Publisher's Note